

Dislocations in P-MBE grown ZnO layers Characterized by HRXRD and TEM

A. Setiawan, I. Hamidah

*Department of Mechanical Engineering and Graduate School of Science Education,
Indonesia University of Education
Setiabudhi 207 Bandung 40154, Indonesia*

T. Yao

*Center for Interdisciplinary Research, Tohoku University
Aramaki, Aoba-ku, Sendai, 980-8578, Japan*

Abstract

We have characterized dislocations in ZnO layers grown on c-sapphire (α -Al₂O₃) by plasma-assisted molecular-beam epitaxy (P-MBE) with and without MgO buffer layer. ZnO without MgO buffer was grown three-dimensionally (3D), while ZnO with MgO buffer was grown two-dimensionally (2D). Mosaic spread (tilt and twist angles) and type and density of dislocations in the layers were studied both by high-resolution X-ray diffraction (HRXRD) and transmission electron microscopy (TEM). HRXRD experiments reveal that screw dislocation densities in the ZnO layer are $8.1 \times 10^8 \text{ cm}^{-2}$ and $6.1 \times 10^5 \text{ cm}^{-2}$, for ZnO with and without MgO buffer, respectively, while edge dislocation densities are $1.1 \times 10^{10} \text{ cm}^{-2}$ and $1.3 \times 10^5 \text{ cm}^{-2}$, for ZnO with and without MgO buffer, respectively. HRXRD and TEM data showed the same result that the major dislocations in the ZnO layers are edge type dislocations running along c-axis. Therefore, HRXRD technique can be applied to characterize dislocations in ZnO layers.

Keywords: ZnO, dislocations, HRXRD, TEM

1. Introduction

ZnO is a direct band energy gap semiconductor ($E_g=3.37 \text{ eV}$ at RT) with a wurtzite structure. The most outstanding feature of ZnO is its large exciton binding energy, 60 meV, which is about three times larger than that of ZnSe and of GaN. Recent reports on the lasing mechanisms of ZnO have shown that ZnO is a promising photonic material for exciton devices in the wavelength ranging from blue to ultraviolet [1-3].

Because of its low cost, large size, and high quality, c-sapphire has been extensively used as substrate for ZnO epitaxy. The greatest disadvantages of ZnO epitaxy on c-sapphire are the large lattice misfits (18%) and thermal mismatch (13%) between ZnO and c-sapphire and the formation of 30°-rotated domains [4]. Consequently, ZnO layers grown on c-sapphire showed a rough surface morphology and poor crystalline quality [4].

In order to overcome the problems caused by the large mismatch between ZnO and c-sapphire substrate, insertion of a buffer layer material which can reduce lattice misfit between ZnO and c-sapphire seems to be a key to obtain high quality ZnO. The growth of double buffer layers consisting of low temperature (LT)-MgO buffer and LT-ZnO buffer followed by a high temperature (HT) annealing has been utilized with success by P-MBE

[5]. Here, the highly mismatched heterointerface of ZnO/ α -Al₂O₃ (18%) is broken up into two much more slightly mismatched interfaces of ZnO/MgO (9%) and MgO/ α -Al₂O₃ (8%) by inserting a MgO layer, which eventually leads to surface adhesion and lateral epitaxial growth. In the present paper, we investigate detailed structural quality of ZnO layers grown on *c*-sapphire with and without MgO buffer layer.

TEM and HRXRD are greatly powerful tools that are utilized in this study. Here, HRXRD has been used to assess the crystal quality of heteroepitaxial layers including tilt and twist angle, and dislocation densities. While two-beam TEM has been used to determine types, density and distribution of dislocation. Tilt and twist angle, and hence dislocation densities, can be evaluated by a series of HRXRD measurements [6-8].

2. Experiment

ZnO layers were grown on *c*-sapphire by P-MBE either with or without MgO buffer. The substrates were degreased in acetone and methanol in ultrasonic cleaner and then chemically etched in a H₂SO₄ (96%): H₃PO₄ (85%)= 3:1 solutions for 15 minutes at 160 °C. Prior to growth, the substrates were thermally cleaned at 750 °C in the preparation chamber for 1 hour. The substrates were then treated in oxygen plasma at 650 °C for 30 minutes in the growth chamber to produce an oxygen terminated *c*- sapphire surface. Oxygen flow rate and plasma power were set to 2.5 sccm and 300 W, respectively. The sample structure was as follows. Firstly, a LT-ZnO buffer was grown at 490 °C on thermally cleaned *c*-sapphire followed by annealing at 750 °C for 3 min. Then, HT-ZnO was grown at 700 °C. In case of ZnO with MgO buffer, LT-MgO buffer was grown at 490 °C followed by LT-ZnO at 490 °C. The thickness of ZnO layers was 450 nm. The whole growth process were monitored by in-situ RHEED. Structural characterization were carried out by HRXRD and cross-sectional TEM. HRXRD experiments were carried out with a Phillips X'Pert MRD diffractometer. TEM experiments were carried out by JEOL JEM 2000 EX-II operated at 200 kV.

3. Results and discussion

Surface morphology

Figure 1 shows RHEED patterns and the corresponding top view AFM images of ZnO layers (a) without and (b) with MgO buffer. ZnO without MgO buffer shows spotty RHEED patterns, indicating 3D growth mode, while ZnO with MgO buffer shows streaky and specular spot RHEED patterns, indicating 2D growth mode. AFM images shows that faceted crystallites with near triangular shape characterize the morphology of ZnO layer without MgO buffer (Fig. 1(a)). Such a surface usually corresponds to the 3D growth mode. In the contrast, the surface of ZnO layer with MgO buffer (Fig. 1 (b)) is atomic flat. Hexagonal islands composed by terrace dominate the surface. This indicate 2D-growth mode. The rms values of surface roughness at 1 μm^2 scan area are 13 nm and less than 1 nm for ZnO layer grown without and with MgO buffer, respectively.

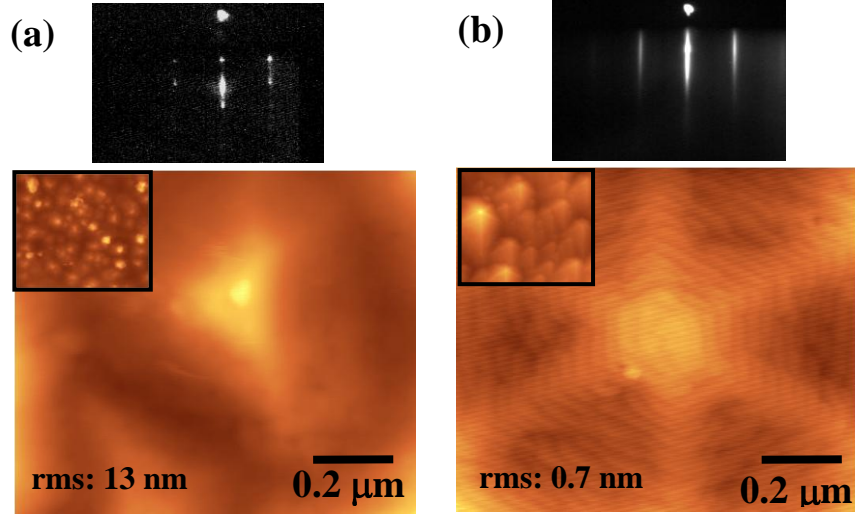


Figure 1. RHEED patterns and corresponding AFM images of ZnO layers grown on c-sapphire (a) without and (b) with MgO buffer. The 10 nm x 10 nm scan area is given in the inset.

Structural quality addressed by HRXRD

In order to address the defect structures of wurtzite ZnO by HRXRD, 0002 Ω - and $10\bar{1}1$ Φ - and Ω - rocking curves measurements were performed. Note that the broadening of 0002 Ω - and $10\bar{1}1$ Φ - rocking curves represent lattice disordering along the growth direction (out of plane) and in-plane disordering, respectively. Figure 2 provides a comparison of (a) 0002 Ω and (b) $10\bar{1}1\Omega$ rocking curves of ZnO layers grown with and without MgO buffer. FWHM values of 0002 Ω scans are 565 arcsec and 18 arcsec, for ZnO grown without and with MgO buffer, respectively. FWHM values of $10\bar{1}1\Omega$ scan are 1346 arcsec and 1076 arcsec, for ZnO films grown without and with MgO buffer, respectively. It should be noted here that FWHM of the 0002 Ω scan was greatly reduced by employing an MgO buffer layer. This directly indicates a small tilt in the c-plane because of the extreme ordering along the growth direction of ZnO(0001) as a consequence of well-controlled layer-by-layer epitaxial growth. Significant broadening of the $10\bar{1}1$ reflection as compared to the 0002 is an indicative of the presence of high edge dislocation density. Note that all type of dislocations (edge, screw, and mixed) broaden the $10\bar{1}1$ reflection, whereas the 0002 reflection is only sensitive to screw and mixed type of dislocations. Furthermore, the FWHM value of the $10\bar{1}1$ Ω scan of the ZnO grown with MgO buffer is smaller than that without MgO, indicating a much lower edge dislocation density.

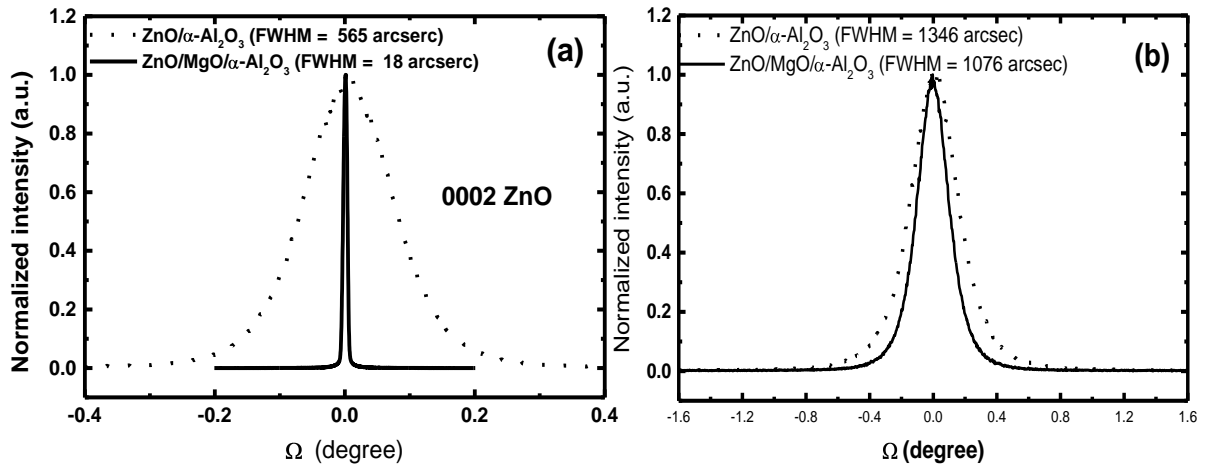


Figure 2. Comparison of (a) 0002Ω and (b) $10\bar{1}1\Omega$ scans of a ZnO layer grown without (*dotted curve*) and with (*solid curve*) MgO buffer.

Mosaic spreads (tilt and twist angles)

Mosaic crystals can be characterized by means of tilt and twist angles and average size of the mosaic blocks. The tilt describes the out-of-plane rotation of the blocks and the twist describes the in-plane rotation. Figure 2 shows the typical Williamson-Hall (W-H) plots for ZnO samples with and without MgO buffer. W-H plot with a linear fit is performed using full width at half maximum (FWHM) of (0002), (0004), (0006) Ω scans, where “FWHM x $\sin(\theta)/\lambda$ ” is plotted against “ $\sin(\theta)/\lambda$ ” in order to determine a tilt angle [8-10]. Here θ is a diffraction angle and λ is a wavelength of $\text{CuK}\alpha$ (0.154056 nm). In the W-H plots, a tilt angle is the slope of the fitted line [8]. From Fig. 2, the tilt angles are determined to be 0.1541° and 0.0056° for the ZnO samples without and with MgO buffer, respectively.

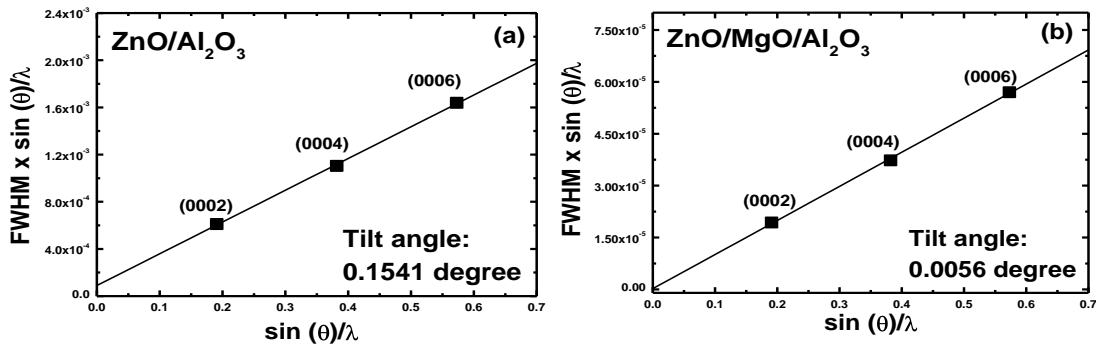


Figure 2. Williamson-Hall plots for a ZnO layer on c-sapphire (a) with and (b) without MgO buffer.

In order to determine the twist angle, FWHMs of (0002), (10-13), (10-12), (10-11), (30-32) Ω scans are plotted as a function of the inclination angles. Figures 3(a) and 3(b) show the plots for ZnO layers without and with MgO buffer, respectively. A twist angle of the samples is determined by estimating the FWHM at an inclination angle of 90° by extrapolation [7]. The dotted curve in Fig. 3 are guiding the eye to the extrapolated FWHM. From Fig. 3, the twist angles are determined to be 0.4387° and 0.4108° , for ZnO without and with MgO buffer, respectively.

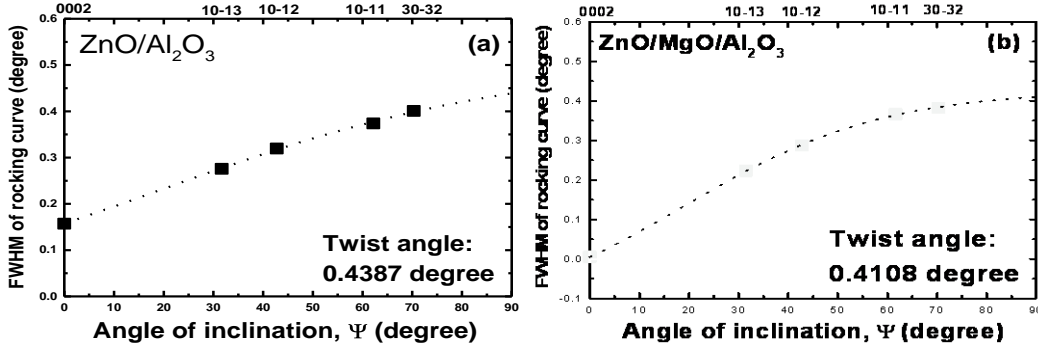


Figure 3. FWHMs of (hkl) Ω rocking curve for reflections (marked at upper x-axis) as a function of inclination angle Ψ of the reflecting lattice planes with respect to the sample surface. (a) ZnO/ α -Al₂O₃ and (b) ZnO/MgO/Al₂O₃.

Types and densities of dislocations accessed by HRXRD

From the determined tilt and twist angles, $\langle 0001 \rangle$ screw and $1/3\langle 11-20 \rangle$ edge dislocations densities are evaluated. Dislocation densities are determined using formalism by Ayers [11], which has been successfully used to determine the dislocation densities in GaN epilayers on sapphire [8,9]. In this formalism, Gaussian shape rocking curve and Gaussian distribution of the orientations of the mosaics are assumed. Dislocation density d is determined using equation of $d = \alpha^2 / (4.35b^2)$, where α is the mosaic angle and \mathbf{b} is the Burgers vector. For the screw dislocation density, the tilt angle and the Burgers vector of $\langle 0001 \rangle$ are used, while the twist angle and the Burgers vector of $1/3\langle 11-20 \rangle$ are used for the edge dislocation density. From the determined tilt angle, screw dislocation densities are determined to be $6.1 \times 10^8 \text{ cm}^{-2}$ and $8.1 \times 10^5 \text{ cm}^{-2}$, for ZnO without and with MgO buffer, respectively. We note that the screw dislocation density of ZnO is greatly reduced, about three-order of magnitude, by employing a MgO buffer. From the determined twist angles, edge dislocations densities are determined to be $1.3 \times 10^{10} \text{ cm}^{-2}$ and $1.1 \times 10^{10} \text{ cm}^{-2}$, for ZnO without and with MgO buffer, respectively. The edge dislocation density is slightly reduced by employing a MgO buffer. Low screw dislocation density in ZnO layer with MgO buffer implies well ordering in the growth direction while the high edge dislocation density means high disordering in the c-plane. The high edge dislocation density is caused by high in plane lattice misfit between ZnO layer and MgO buffer. Table 1 summarizes tilt and twist angles, and dislocation densities determined by HRXRD and TEM.

Table 1. Tilt and twist angle and dislocation densities.

Parameter	ZnO without MgO buffer	ZnO with MgO Buffer
Tilt angle (degree)	0.1541	0.0056
Twist angle (degree)	0.4387	0.4108
<0001> screw dislocation (cm ⁻²)	6.1 x 10 ⁸	8.1 x 10 ⁵
<11-20> edge dislocation (cm ⁻²)	1.3 x 10 ¹⁰	1.1 x 10 ¹⁰
TEM: Dislocations density (cm ⁻²)	6 x 10 ¹⁰	2 x 10 ¹⁰

Types and densities of dislocations accessed by TEM

Types of dislocation in the ZnO samples were characterized by cross-sectional TEM under two-beam condition, as shown in Figure 4. The samples were observed near the [2-1-10] zone axis with diffraction vectors $\mathbf{g} = [0006]$ (Fig. 4(a) and Fig. 4(c)) and $\mathbf{g} = [03-30]$ (Fig. 4(b) and Fig. 4(d)). By invisibility criterion, screw-type dislocations should be visible under $\mathbf{g} = 0006$ and invisible under $\mathbf{g} = 03-30$. In the contrast, edge-type-dislocations should be invisible under $\mathbf{g} = 0006$ and visible under $\mathbf{g} = 03-30$. Mixed-type dislocations should be visible under both of the \mathbf{g} vectors. By averaging several pictures, for ZnO layer with MgO buffer, threading dislocations were roughly distributed as 31% of screw-type (Burgers vectors $\mathbf{b} = [0001]$), 61% of edge-type (Burgers vectors $\mathbf{b} = 1/3\langle 11-20 \rangle$), and 8% of mixed-type (Burgers vectors $\mathbf{b} = 1/3\langle 11-23 \rangle$) dislocations. For ZnO with MgO buffer, threading dislocations were distributed as 98% of edge-type and 2% of screw-type and mixed type dislocations. Here, major threading dislocations running along c-axis are edge-type dislocation with Burgers vector of $1/3\langle 11-20 \rangle$ in both the samples. Comparison of Fig. 4(a) and Fig. 4(c) reveals that the screw dislocations are greatly reduced by introducing the MgO buffer. From plane-view TEM images (data are not shown here), Total dislocation densities were determined to be $6 \times 10^{10} \text{ cm}^{-2}$ and $2 \times 10^{10} \text{ cm}^{-2}$, for ZnO layers without and with MgO buffer, respectively.

Figure 4 shows another important fact. At the interface region, a high density of interfacial threading dislocations was observed. Surprisingly, the dislocation density rapidly decreases beyond 20 nm. Furthermore, by increasing layer thickness the density of threading dislocation in ZnO with MgO buffer decrease faster than that of without MgO buffer. It can only be understood if these threading dislocations are not along the c-axis so that they strongly interact with each other and annihilated quickly [12]. Since favorable dislocation in MgO with fcc lattice is not along c-axis, much stronger interaction between dislocations might be introduced when ZnO initially nucleated on a MgO which lead to reduce dislocation density. Furthermore, lattice misfit between ZnO and MgO (9%) is smaller than between ZnO and c-sapphire (18%). Therefore, the density of interfacial defect in ZnO with MgO buffer is smaller that that of without MgO buffer.

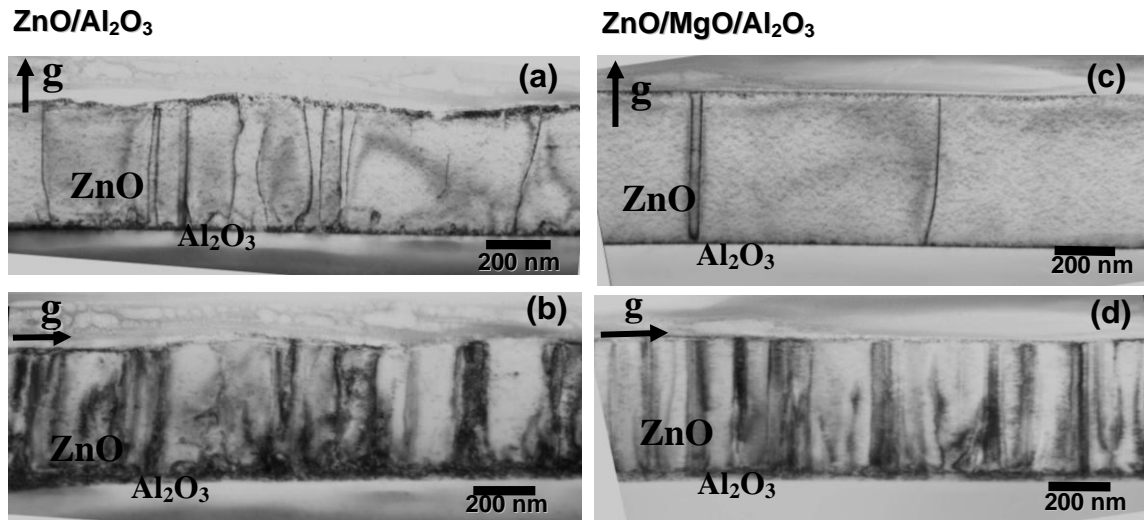


Figure 4. Two beam bright-field cross-sectional electron micrographs of the ZnO/ α -Al₂O₃ and ZnO/MgO/ α -Al₂O₃ near the [2-1-10] zone axis with $g = 0006$ ((a) and (c)) and $g = 03-30$ ((b) and (d)).

4. Conclusions

We have studied dislocations in ZnO layers grown on α -Al₂O₃ by P-MBE with and without MgO buffer layer. Mosaic spread (tilt and twist angles), type and density of dislocations in layers were characterized by high-resolution X-ray diffraction (HRXRD) and the results were compared with Transmission electron microscopy (TEM) data. Screw dislocation densities in ZnO layer determined by HRXRD are $8.1 \times 10^8 \text{ cm}^{-2}$ and $6.1 \times 10^5 \text{ cm}^{-2}$, for ZnO with and without MgO buffer, respectively, while edge dislocation densities in ZnO layer are $1.1 \times 10^{10} \text{ cm}^{-2}$ and $1.3 \times 10^5 \text{ cm}^{-2}$, for ZnO with and without MgO buffer, respectively. HRXRD and TEM data showed the same results that the major dislocations in the ZnO layers are edge type dislocations running along c-axis. Those values of dislocation densities are agree with TEM data. Therefore, HRXRD technique can be applied for dislocations characterization of ZnO layers.

Acknowledgements

The author would like to thank Prof. S.K. Hong, Dr. H. J. Ko, and Dr. Yefan Chen for their useful discussions on P-MBE growth. The author also would like to thank Directorate general of Higher Education of Indonesia for its financial support under Fundamental Reserch Project (contract number: 014/DP2M/II/2006).

References

- [1] D.M. Bagnall, Y.F Chen, Z. Zhu, T. Yao, S. Koyama, M. Y. Shen, and T. Goto, "Optically pumped lasing of ZnO at room temperature", *Appl. Phys. Lett.* **70**, American Institute of Physics, 28 April 1997, pp. 2230-2232.
- [2] D.M. Bagnall, Y.F Chen, Z. Zhu, T. Yao, M.Y. Shen, and T. Goto, "High temperature excitonic stimulated emission from ZnO epitaxial layers", *Appl. Phys. Lett.* **73**,

- American Institute of Physics, 24 August 1998, pp. 1038-1040.
- [3] H. J. Ko, Y. F. Chen, K. Miyajima, A. Yamamoto and T. Goto, “Biexciton emission from high-quality ZnO films grown on epitaxial GaN by plasma-assisted molecular beam epitaxy”, *Appl. Phys. Lett.* **77**, American Institute of Physics, 24 July 2000, pp.537-539.
- [4] P. Fons, K. Iwata, A. Yamada, K. Matsubara, S. Niki, K. Nakahara, T. Tanabe, H. Takasu, “Uniaxial locked epitaxy of ZnO on the *a* face of sapphire”, *Appl. Phys. Lett.* **77**, American Institute of Physics, 18 September 2000, pp.180-18031.
- [5] Y.F. Chen, H.J. Ko, S.K. Hong, T. Yao, *Appl. Phys. Lett.* **76**, American Institute of Physics, 31 January 2000, pp. 559-561.
- [6] V. Srikant, J. S. Speck, and D. R. Clarke, , “Mosaic structure in epitaxial thin films having large lattice mismatch” *J. Appl. Phys.* **82**, American Institute of Physics, 1 November 1997, pp.4286-4295.
- [7] H. Heinke, V. Kirchner, S. Einfeldt, and D. Hommel, “X-ray diffraction analysis of the defect structure in epitaxial GaN”, *Appl. Phys. Lett.* **77**, American Institute of Physics, 2 October 2000, pp. 2145-2147.
- [8] T. Metzger, R. Hopler, E. Born, O. Ambacher, M. Stutzmann, R. Stommer, M. Stutzmann, R. Stommer, M. Schuster, H. Gobel, S. Christiansen, M. Albrecht, and H.P. Strunk, Defect structure of epitaxial GaN films determined by transmission electron microscopy and triple-axis X-ray diffractometry“, *Phil. Mag. A* **77**, Taylor and Francis Ltd, 1998, pp.1013-1025.
- [9] G. K. Williamson and W.H. Hall, “X-ray line broadening from filed aluminium and wolfram” *Acta Metall.* **1**, January 1953, pp.22 -31.
- [10] Soon-Ku Hong, Hang-Ju Ko, Yefan Chen, and T. Yao, “Structural characterization of P-MBE grown ZnO epilayers on GaN/Al₂O₃ by HRHRD” (Unpublished).
- [11] J. E. Ayers, “The measurement of threading dislocation densities in semiconductor crystals by X-ray diffraction”, *J. Crystal Growth* **135**, Elsevier Science, North-Holland, 1994, pp. 71-77.
- [12] Y. F. Chen, S. K. Hong, H. J. Ko, V. Kirshner H. Wenis, T. Yao, K. Inaba, and Y. Segawa, “Effect of extremely thin buffer on heteroepitaxy with large lattice mismatch”, *Appl. Phys. Lett.* **78**, American Institute of Physics, 21 May 2001, pp. 3352-3354.